PHYSICS AND CHEMISTRY
OF SOLID STATE
V.21, No.2 (2020) pp. 219-226

DOI: 10.15330/pcss.21.2.219-226

Vasyl Stefanyk Precarpathian
National University

ФІЗИКА І ХІМІЯ ТВЕРДОГО ТІЛА
Т. 21, № 2 (2020) С. 219-226

PACS 82.45.Aa, 81.05.Uw, 82.47.Uv

ISSN 1729-4428

B.K. Ostafiychuk[1], H.M. Kolkovska[1], B.I. Rachiy[1], P.I. Kolkovskyi[1],
I.P. Yaremiy[1], N.Ya. Ivanichok[1], S.I. Yaremiy[2]

Synthesis and Electrochemical Properties of $LaMnO_3$ Perovskite Nanoparticles

[1]Vasyl Stefanyk Precarpathian National University, Ivano-Frankivsk, Ukraine, Pkolkovskyy@gmail.com
[2] Ivano-Frankivsk National Medical University, Ivano-Frankivsk, Ukraine,

In this work, the perovskite $LaMnO_3$ material has been prepared based on the sol-gel process of synthesis with the participation of combustion. According to the X-ray phase analysis, it was determined that the obtained material consists of $LaMnO_3$ one phase (space group Pm-3m). Nevertheless, it has been determined that the average size of the coherent scattering region of the obtained material is about 24 nm. Moreover, the average particle size is 40 - 60 nm in case the approximation that the particles are spherical shape. Thus, it has been determined that the specific surface area of the material is 42 m^2/g. The electrochemical investigations have been performed using nanosized $LaMnO_3$ powder as a cathode material for electrochemical capacitors. The $LaMnO_3$ material under research showed a specific capacity of 40 F/g at a discharge of up to 1V.

Keywords: sol-gel process, perovskite structure, KOH electrolyte, specific capacity.

Received 30 April 2020; Accepted 15 June 2020.

Introduction

Much attention today is paid to the development of new and improvement of existing electrochemical current sources. One of the most optimal storage of electrical energy is electrochemical capacitors (EC). For the optimal use of EC in practice, it is necessary to increase the value of their specific energy and power and reduce the technological cost of the system. The solution to this problem is the development of hybrid electrochemical capacitors, which are a battery-capacitor electrochemical system that can solve the problems of increasing the specific energy of the EC and the specific power and limited charge / discharge cycles in lithium-ion current sources [1, 2].

The increase in capacity and stability of the charge-discharge cycle are the main reasons for the search for new electrode materials for electrochemical capacitors. One of the materials that correspond to these qualities are materials with a perovskite structure of the general formula ABO_3, where position A contains alkaline earth metals, such as Lanthanum, and position B contains transition metals having 6-fold coordination [3]. A feature of the perovskite structure is its ability to possible combinations with fragments of other structures, as a result of which new frame or layered composite structures can arise and their characteristics can significantly improve [4]. Also, materials of this type are widely research as functional materials of electronic technology, laser materials, sensors, catalysts [5] and materials for solar cells [6].

The oxidation state of cations A and B are depend on the structure of the perovskite material and allows changing the properties of this material [7]. A change in the oxidation state of metal oxide in the structure of perovskite allows the use of these materials as electrode materials for supercapacitors [8]. One of the most promising transition metal oxides is MnO_2 nanoparticles, which have high thermal and structural stability, low cost and ease of processing. [8, 9, 10]. Recently, considerable attention has been paid to perovskite, as electrode materials for supercapacitors, due to the mechanisms of oxygen-anion intercalation of charge accumulation, significantly affects the electrochemical parameters of electrodes [11]. Among the most promising cathode materials of this type is $LaMnO_3$, which is characterized by environmental and economic availability and fairly high electrochemical parameters [12, 13]. Oxygen vacancy is an important characteristic of the structure of perovskite material and significantly affects the specific capacitance of $LaMnO_3$ nanoparticles [12]. Therefore, these materials, due to oxygen vacancies and fast ion diffusion, have been used as electrode materials in energy storage [14].

It was determine that a slight substitution of position A in $LaMnO_3$ perovskite systems with a lower valence cation (Sr^{2+}) creates electron holes at position B. In $LaMnO_3$ perovskite systems, to maintain the electroneutrality condition, Mn^{3+} can be oxidized to Mn^{4+}, which leads to an increase in electronic conductivity [15, 16] and improves electrochemical values.

The electrochemical properties of perovskite material are depending on the concentration and type of electrolyte ions. With an increase in the concentration of electrolyte ions, an increase in oxygen vacancies is observed, which in turn strengthens the pseudocapacity characteristics of materials with perovskite structure [17, 18].

Materials with a perovskite structure are capable of energy storage well due to reverse Faraday processes [12, 19]. However, the main drawback of the $LaMnO_3$, as an electrode material for electrochemical capacitors is the low conductivity and short charge/discharge cycle [13, 19].

I. Experimental details

LaMnO3 complex oxide was obtained by the sol-gel method with the participation of auto-mine. The synthesis reagents were lanthanum nitrate ($La\ (NO_3)_3 \cdot 6H2O$), manganese nitrate ($Mn\ (NO_3)_2 \cdot 6H_2O$) and citric acid ($C_6H_8O_7 \cdot H_2O$). The stoichiometric redox reaction between the fuel and the oxidizing agent was based on the molar ratio of metal nitrates to citric acid 1: 1.

The first stage of the synthesis was the corresponding amount of metal nitrates and citric acid were dissolved in distilled water. To establish a pH = 7, a small amount of a 25 % aqueous ammonia solution was added to the resulting solution, thereby obtaining a milky pink solution. The resulting sol was placed in an furnace at 400 K for 10 - 12 hours until completely dry. During the dehydration process, a polycondensation reaction took place between citric acid and metal nitrates to form a gel. After complete drying, the obtained material was heated to 570 K. After a few minutes, the process of auto-xerogel xing took place, as a result of which the bulk material LaMnO3 was obtained.

The microstructure of LaMnO3 samples was investigated using a scanning electron microscope (SEM).

The phase composition and crystal structure of the obtained materials were investigated by XRD based on DRON – 3 M diffractometer (Cu Kα radiation). The diffraction patterns were processed by the full-profile Rietveld analysis using the FullProf program. The size of the nanocrystallites of the sample and its phase composition were determined based on the X-ray structural analysis.

The characteristics of the obtained sample (surface area and total pore volume) of the $LaMnO_3$ perovskite material were determined based on the analysis of nitrogen adsorption / desorption isotherms at boiling point (77 K) by Quantachrome Autosorb Nova 2200e instrument. Namely, the total surface area (SBET) by the BET multipoint method in the isotherm limited by the relative pressure range P/P0 = 0.050...0.35. The total pore volume (Vtotal, cm^3/g) calculated by the amount of sorbet nitrogen at P/P0 ~ 1. Additionally, the samples were previously degassed at 470 K for 18 h.

Electrochemical measurements were performed based on three - electrode cells consisted of working electrode (electrode composition on the pure Ni subtract 1 cm^2) reference electrode (Ag / AgCl), counter electrode (platinum wire). Electrode composition consists of 85 % active material, 10 % acetylene black and 5 % polyvinylidene fluoride mixed with n-methylpyrrolidone and dried at 300 K for 3 hours. 6 M KOH was used as an electrolyte. Electrochemical investigation were performed an Autolab PGSTAT/FRA-2 spectrometer in galvanostatic and potentiodynamic modes.

II. Results and discussion

The sol-gel method based on the participation of auto combustion, which is used for the synthesis of nanosized powders, has several advantages compared to other methods, since it does not require complex and expensive equipment or rare reagents for synthesis. The technology and synthesis features of the studied material are described in [20]. The $LaMnO_3$ compound is formed as a result of a chemical reaction:

$$36La\ (NO_3)_3 \cdot 6H_2O + 36Mn\ (NO_3)_2 \cdot 6H_2O + 50C_6H_8O_7 \cdot H_2O \xrightarrow{NH_3 \cdot H_2O} 36LaMnO_3 + 90N_2 \uparrow + 300CO_2 \uparrow + 682H_2O \uparrow \quad (1)$$

Typical SEM images of the surface of the obtained material at various magnifications are shown in Fig. 1. It was established that the synthesized $LaMnO_3$ has a mesoporous structure with particle sizes of 40 - 60 nm. With high-resolution SEM images, a clear crystallinity of the obtained material is seen. Fig. 2 a show the nitrogen adsorption-desorption isotherms are presented by $LaMnO_3$ material. Using the BET method, the specific surface area of the synthesized material was determined, which is 42 m^2/g. The pore size distribution according to the BJH method is shown in Fig. 2b. The material is mesoporous with a cavity size of 5 to 12 nm. The results

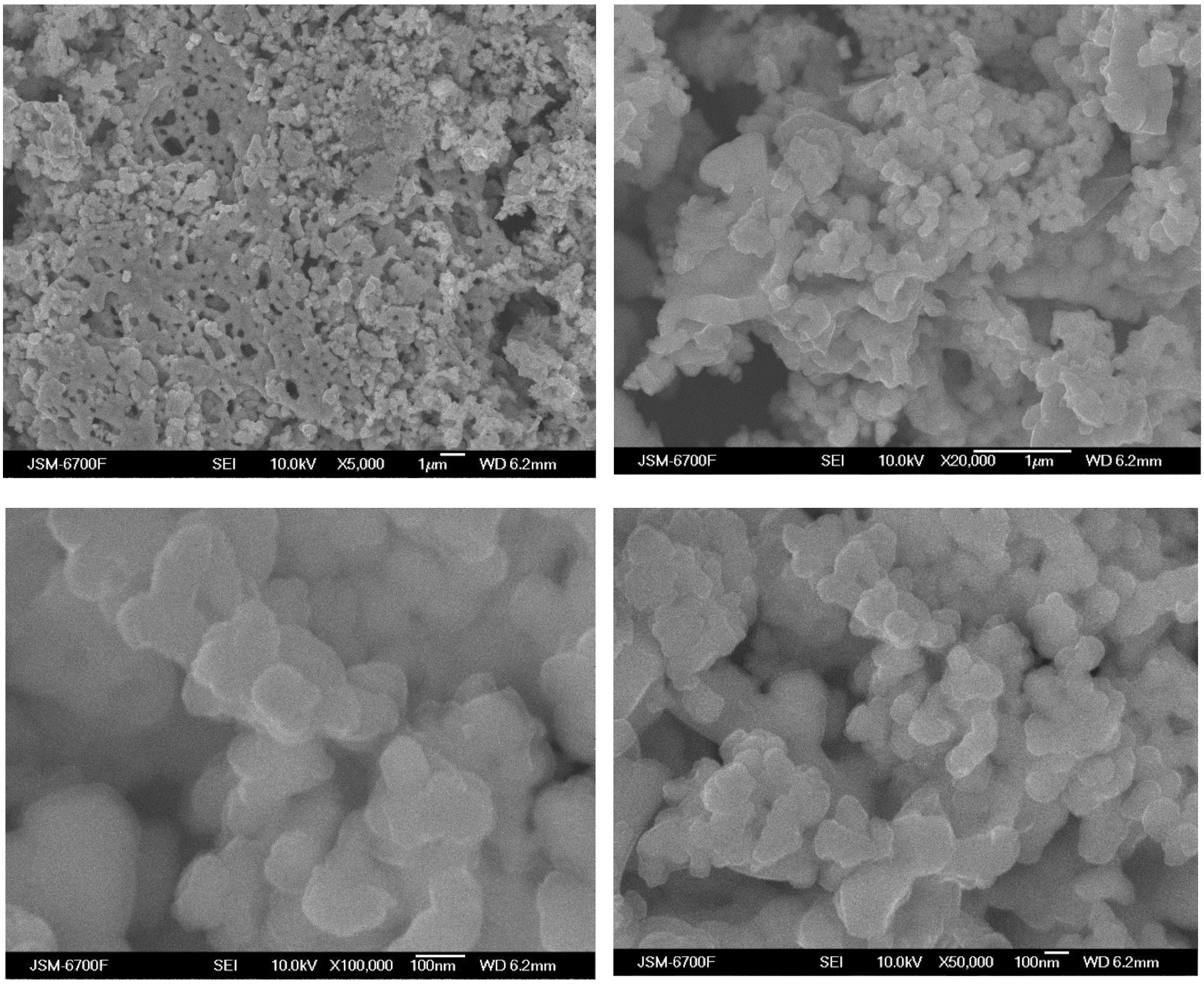

Fig. 1. SEM micrographs of $LaMnO_3$..

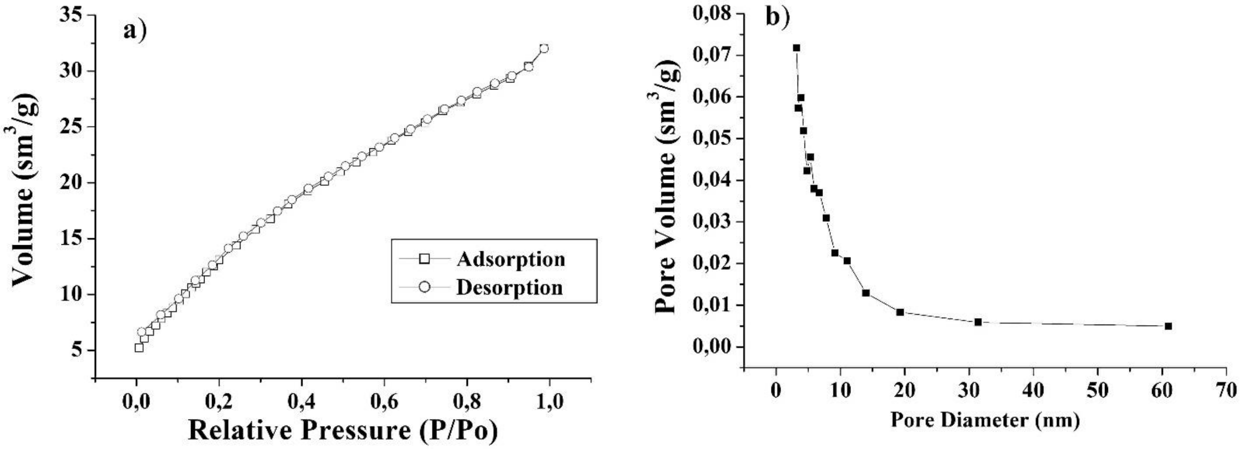

Fig. 2. N_2 adsorption-desorption isotherm a) and pore size distribution of $LaMnO_3$ b).

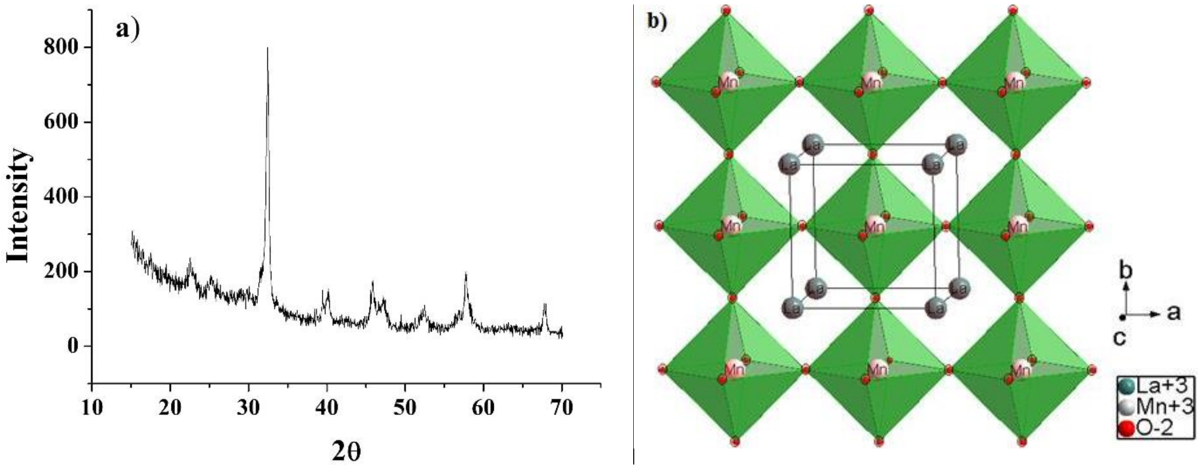

Fig. 3. Diffraction patterns of $LaMnO_3$ material (a) and model of the crystal structure of $LaMnO_3$ (view along the C axis) (b).

obtained indicate that the mesoporous structure of the $LaMnO_3$ material is favorable for the diffusion of electrolyte ions.

If we assume that the particles of the formed phase have a spherical shape, then the average particle diameter d_c and the specific surface area S_n are related by the relation: $d_c = 6/\ \rho S_n$ where ρ is the density of the material. It was determined that the average particle size is 22 ± 2 nm based on the obtained X-ray density of the synthesized material and the measured specific surface area by the BET method. Thus, we can assume that the synthesized material consists of particles of a size of 20 nm, which are aggregated into particles of a size of 50 - 60 nm.

Fig. 3a shows the diffraction patterns of the obtained $LaMnO_3$. From the experimental X-ray diffraction pattern, it was determined that the peak diffraction (2θ = 23, 32, 40, 46, 52, 58, 68) for the obtained material is well indexed with the cubic phase of pure $LaMnO_3$. Thus, we can assume that the investigated material has a perovskite structure of the space group Pm - 3m. Figure 3b shows a model of the crystal structure of synthesized $LaMnO_3$ (view along the c axis), from which it can be seen that the Mn cation is in the octahedral environment of O^{2-} anions. According to the simulation data, it was established that the formed Mn – O bonds in the equatorial plane and axial vertices have a length of about 1.944 Å, and the length of the O – O bonds for axial vertices is about 2.7492 Å. La ions are placed between the equally oriented octahedron. The coordination polyhedron has the shape of a cuboctahedron.

The lattice constant of the synthesized material is a = 3.945 Å, and the volume is V = 61.38 Å^3. According to the X-ray analysis, the density of the material is $\rho = 6.54$ g/cm^3. The average size of the coherent scattering regions is 24 nm.

The electrochemical characteristics of the synthesized $LaMnO_3$ material were research using cyclic voltammetry in the potential range 0 - 1 V with respect to the Ag/AgCl reference electrode in the range of scan rates of 1 - 20 mV/s. When the electrode is cycled based on the $LaMnO_3$ material under research in the potential range (0 - 1 V), its capacitance is provided by negative electrolyte ions (OH groups).

Fig. 4 shows the obtained CVA curves for the $LaMnO_3$ sample at a scan rate of 1 mV/s, which are asymmetric. The curves are characterized by peaks that are responsible for the oxidation of Mn ions. Peaks corresponding to oxidation and reduction processes are observed both on the anode and cathode branches, respectively. The peak at 0.4 V corresponds to the oxidation of Mn^{2+} to Mn^{3+} due to the intercalation of oxygen ions in an oxygen vacancy [12].

The peak observed at 0.85 V is a consequence of the intercalation of excess oxygen into the structure at which Mn^{3+} is oxidized to Mn^{4+}. Thus, it can be argued that the contribution to the capacity of the material under study is

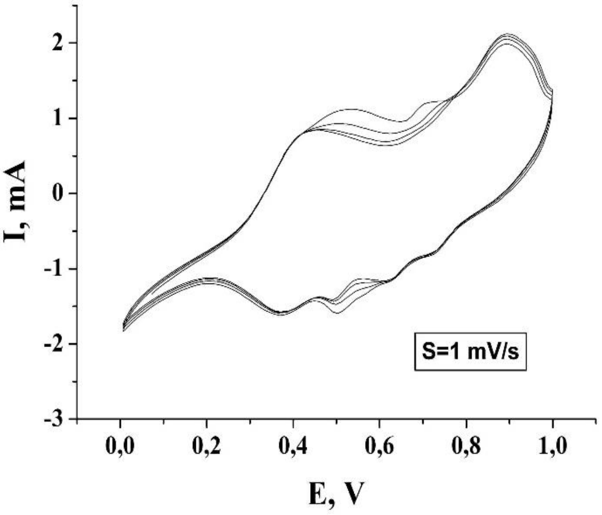

Fig. 4. CVA curves of the $LaMnO_3$/KOH system at s = 1mV/s.

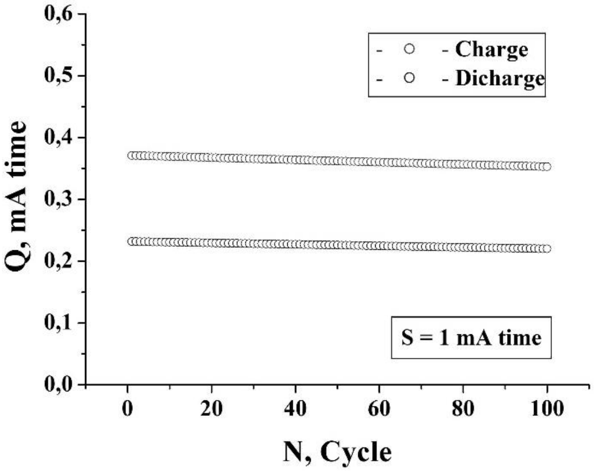

Fig. 5. Specific capacity of $LaMnO_3$ depending on the number of charge/discharge cycles

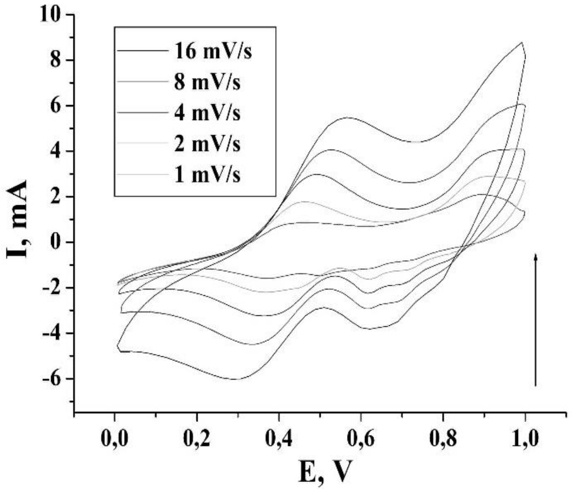

Fig. 6. CVA curves of the $LaMnO_3$/KOH system at 1 to 16 scan rates.

provided mainly by redox reactions and an insignificant contribution of the charge that accumulates as a result of the formation of a double electric layer (DEL).

Using voltammograms, the dependence of the specific capacitance of $LaMnO_3$ material on the cycle number was determined (Fig. 5). The structure is stable, as evidenced by the independence of the value of the accumulated charge during long cycling. With an increase in the scan rates from 2 to 16 mV / s (Fig. 6) on the voltammogram, the anode peaks shift towards high potentials by about 0.15 V, the cathode peak shift is insignificant and amounts to 0.02 - 0.05 V. At maximum scan rate on the voltammogram maintains the presence of peaks, which indicates the progress in the system of fast reverse Faraday redox / reduction processes, however, the internal electrical resistance of the system is growing, due to the mobility of electrolyte ions.

The dependence of the specific capacity of the obtained $LaMnO_3$ material on the scan rate is shown in Fig. 7. The maximum value of the specific capacity of the system under research is 40 F/g at a scan rate of 1 mV/s.

Figure 7 shows that with increasing scan rate, the capacity of the material decreases. Using the obtained dependence of *C* on *s*, the total capacity of the material under research can be divided into the capacity of a double electric layer (C_{DEL}) and the diffusion-controlled redox capacity due to the faraday reverse redox (C_F) reactions: $C = C_{DEL} + C_F$ [21]. In the kinetic model [21], it is assumed that the scan rate affects the total specific electrochemical capacitance of the system, since the diffuse component of the capacitance (C_F) is a function of the reaction time.

So, the scan rate can be considered inverse to the time of diffusion. Thus, in the case of linear diffusion, the total capacitance is related to the scan rate by the following equation: $C = C_{S=\infty} + a/\sqrt{s}$ where *a* is a constant value, a. $C_{DEL} = C_{S=\infty}$ As follows from fig. 8, the specific capacity of $LaMnO_3$ material linearly depends on $s^{-1/2}$. Extrapolation of the *C* dependences from $s^{-1/2}$ to the Y axis (Fig. 8) made it possible to determine the

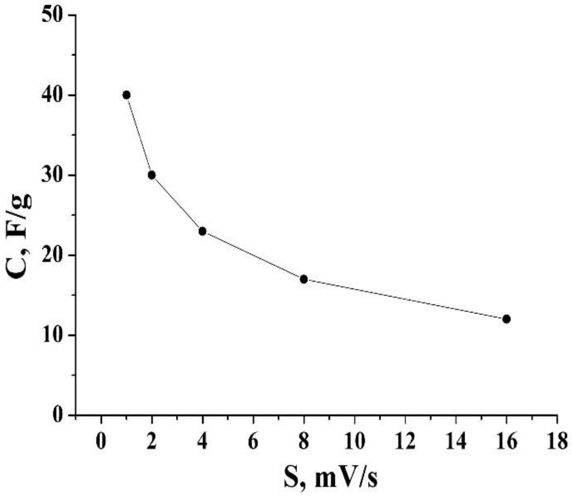

Fig. 7. Specific capacity of the $LaMnO_3$/KOH system.

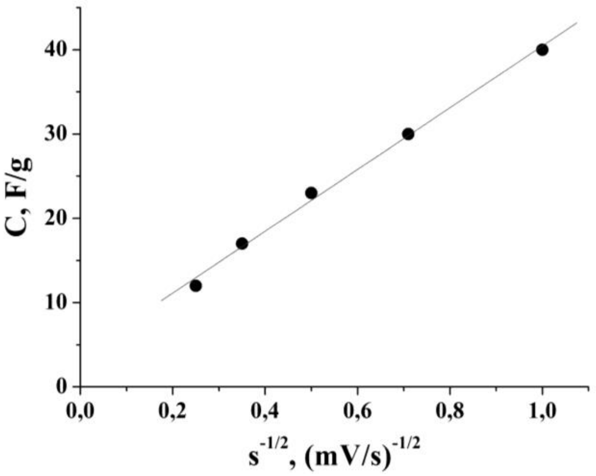

Fig. 8. Dependence of specific capacity on $s^{-1/2}$.

Table 1

Specific capacitive characteristics of $LaMnO_3$/KOH System

C_F, F/g	180
C_{max}, F/g	185
C_F/C_{max}	0.97

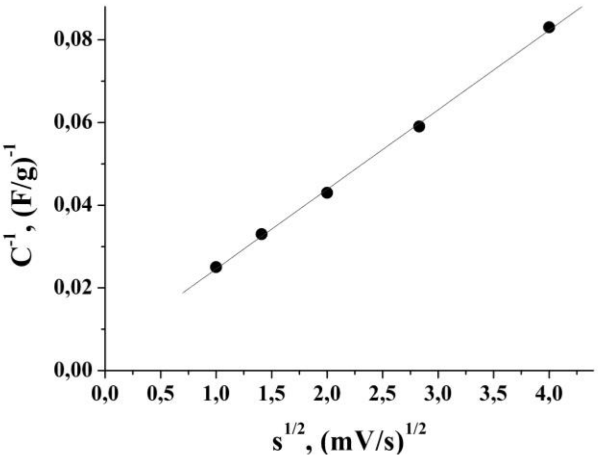

Fig. 9. Dependence of C^{-1} on $s^{1/2}$ for $LaMnO_3$.

specific capacity of the DEL of the materials under research (Table 1).

The dependence of the specific capacitance on the scan rate can be extrapolated to the other side to s = 0 using the functional dependence on s. Since *C* grows linearly with $s^{1/2}$, then *1/C* should decrease linearly with s1/2. Then, $1/C = 1/C_{x=0} = b\sqrt{s}$ where the maximum specific capacity that can be obtained, *b* is a constant value (Fig. 9).

As follows from Fig. 9, the reciprocal of the specific capacitance linearly depends on $s^{1/2}$. The extrapolation of the dependences of C^{-1} on $s^{1/2}$ of the Y axis (Fig. 9) made it possible to determine the maximum specific capacity of the material under study (Table 1).

The charge-discharge curves of an electrochemical system with $LaMnO_3$-based electrodes are shown in Fig. 10. The discharge curves are characterized by two linear sections with different tilt angles, which indicate two different mechanisms of electric energy storage. For a proper assessment of the amount of charge stored on the electrode, the specific capacitance Cm is used, which can be calculated by the formula: $C_m = \frac{C}{m} = \frac{I\times\Delta t}{\Delta U\times m}$ where C_m (F/g) is the specific capacity, *I* (mA) is the discharge current, *Δt* (s) is the discharge time, *ΔU* (V) is the potential during the discharge, and *m* (g) is the mass of the active material inside the electrode.

The capacitance characteristics of the $LaMnO_3$ electrode material at various discharge currents are shown in Fig. 11. At a discharge current of 1 mA, the specific capacity is 62 F/g. It can be seen from the figure that, with an increase in the discharge current, the capacitance of the electrode material $LaMnO_3$ significantly decreases. This is probably due to the fact that, at high discharge currents, there is not enough time for the electrolyte ions to completely penetrate into the electrode materials and enter vacancies.

Conclusions

The complex oxide of $LaMnO_3$ was obtained based on sol-gel method with the participation of auto combustion. It was determined that the obtained material has a perovskite structure of the Pm-3m space group with a lattice parameter of 3.945 Å. The density of the material is 6.54 g/cm^3. Moreover, It was determined that the average size of the coherent scattering regions is 24 nm.

The specific surface area of the synthesized material, determined using the BET method, is 42 m^2/g. The morphology of the material was research and it was determined that the synthesized $LaMnO_3$ is formed by particles with sizes of 40-60 nm, between which cavities from 5 to 12 nm are formed.

The electrochemical investigations of the

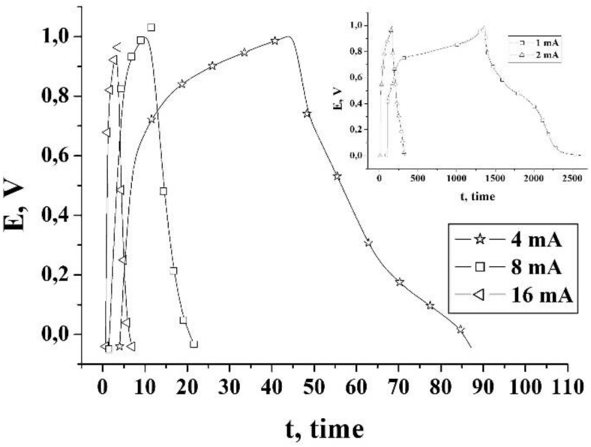

Fig. 10. The charge-discharge curves in the potential window from 0 to 1 V at various currents.

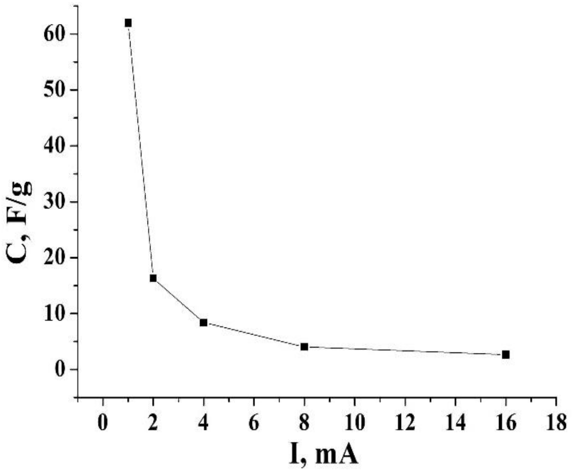

Fig. 11. The density of the specific capacitance of $LaMnO_3$ material measured from the charge-discharge curves of the discharge current.

$LaMnO_3$/electrolyte system were carried out and the dependence of the specific capacity of the obtained material on the rate of change of the potential was determined. It is shown that the total capacity of the material is ensured by the occurrence of redox reactions. The specific capacitance of the $LaMnO_3$ material, calculated according to the data of the potentiodynamic method, is 40 F/g at a scan rate of 1 mV/s. The data obtained are confirmed by the charge/discharge method.

Ostafiychuk B.K. - Doctor of Sciences, Professor, Head of the Department of Material Science and New Technology;
Kolkovska H.M. – PhD student, of the Department of Material Science and New Technology;
Yaremiy I.P. - Doctor of Sciences, Professor, of the Department of Material Science and New Technology;
Rachiy B.I. - Doctor of Sciences, Professor, of the Department of Material Science and New Technology;
Kolkovskyi P.I. – Doctoral student of the Department of Material Science and New Technology;
Ivanichok N. Ya – PhD, senior specialist of the Department of Material Science and New Technology;
Yaremiy S.I. – PhD, teacher of the Department of Medical Informatics, Medical and Biological Physics.

[1] W. Zhe, Y. Su, D. Wang, F. Li, J. Du, H. Cheng, Advanced Energy Materials 1(5), 917 (2011) (https://doi.org/10.1002/aenm.201100312).
[2] R. Lisovsky, B. Ostafiychuk, I. Budzulyak, V. Kotsyubynsky, A. Boychuk, B. Rachiy, Acta Physica Polonica A 133(4), 876 (2018) (doi: 10.12693/APhysPolA.133.876).
[3] E. Arendt, A. Maione, A. Klisinska, O. Sanz, M. Montes, S. Suarez, J. Blanco, P. Ruiz, Applied Catalysis A: General 339(1), 1 (2008) (https://doi.org/10.1016/j.apcata.2008.01.016).
[4] D. Munoz, N.M. Harrison, F. Illas, Physical Review B, 69, 8 (2004) (https://doi.org/10.1103/PhysRevB.69.085115).
[5] S.A. Veldhuis, P.P. Boix, N. Yantara , M. Li, T.C. Sum, N. Mathews, S.G. Mhaisalkar, Advansed Materials 28(32), 6804 (2016) (https://doi.org/10.1002/adma.201600669).
[6] N. G. Park, Materials today, 8(2), 65-72 (2015) (https://doi.org/10.1016/j.mattod.2014.07.007).
[7] P.M. Wilde, T.J. Guther, R. Oesten, J. Garche, Journal of Electroanalytical Chemistry 461(1-2), 154 (1999) (https://doi.org/10.1016/S0022-0728(98)00179-X).
[8] L. Hehe, X. Zhang, R. Ding, L. Qi, H. Wang, Electrochimica Acta 108, 497 (2013) (https://doi.org/10.1016/j.electacta.2013.07.066).
[9] B.K. Ostafiychuk, M.I. Kolkovskyi,, B.I. Rachiy, P.I. Kolkovskyi, N.Y. Ivanichok, R.V. Ilnitsky, Physics and Chemistry of Solid Stat 21(1), 19 (2020) (https://doi.org/10.15330/pcss.21.1.19-34).
[10] Y. Hu, J. Wang, Journal of Power Sources 286, 394 (2015) (https://doi.org/10.1016/j.jpowsour.2015.03.177).
[11] H. Nan, X. Hu, H. Tian, Materials Science in Semiconductor Processing 94, 35 (2019) (https://doi.org/10.1016/j.mssp.2019.01.033).
[12] J.T. Mefford, W.G. Hardin, S. Dai, K.P. Johnston, K.J. Stevenson, Nature Materials 13, 726 (2014) (https://doi.org/10.1038/nmat4000).
[13] X. Wang, Q. Zhu, X. Wang, H. Zhang, J. Zhang, L. Wang, Journal of Alloys and Compounds 675, 195 (2016) (https://doi.org/10.1016/j.jallcom.2016.03.048).
[14] K. Zhang, X. Han, Z. Hu, X. Zhang, Z. Tao, J. Chen, Chemical Society Reviews 44 (3), 699 (2015) (https://doi.org/10.1039/C4CS00218K).
[15] A. Mahata, P. Datta, R.N. Basu, Ceramics International 43(1), 433 (2017) (https://doi.org/10.1016/j.ceramint.2016.09.177).
[16] Z.A. Elsiddig, H. Xu, D. Wang, W. Zhang, X. Guo, Y. Zhang, Zh. Sun, J. Chen, Electrochimica Acta 253, 422 (2017) (https://doi.org/10.1016/j.electacta.2017.09.076).
[17] K.C. Tsay, L. Zhang, J. Zhang, Electrochimica Acta 60, 428 (2012) (https://doi.org/10.1016/j.electacta.2011.11.087).
[18] B.K. Ostafiychuk, I.M. Budzulyak, B.I. Rachiy, R.P.Lisovsky, V.I. Mandzyuk, P.I. Kolkovsky, R.I. Merena, M.V. Berkeshchuk, L.V. Golovko, Journal of Nano- and Electronic Physics 9(5), 05001 (2017) (DOI: 10.21272/jnep.9(5).05001).
[19] Y. Cao, B. Lin, Y. Sun, H. Yang, X. Zhang, Electrochimica Acta 174, 41 (2015) (https://doi.org/10.1016/j.electacta.2015.05.131).
[20] Y. Li, L. Xue, L. Fan, Y. Yan, Journal of Alloys and Compounds 478(1-2), 493 (2009) (https://doi.org/10.1016/j.jallcom.2008.11.068).
[21] M.W. Xu, L.B. Kong, W.J. Zhou, H.L. Li, Journal of Physical Chemistry C 111(51), 19141 (2007) (https://doi.org/10.1021/jp076730b).

Б.К. Остафійчук[1], Г.М. Колковська[1], І.П. Яремій[1], Б.І. Рачій[1],
П.І. Колковський[1], Н.Я. Іванічок[1], С.І. Яремій[2]

Синтез та електрохімічні властивості нанорозмірного перовскитного матеріалу $LaMnO_3$

[1]*ДВНЗ "Прикарпатський національний університет імені Василя Стефаника", Івано-Франківськ, Україна,*
Pkolkovskyy@gmail.com
[2]*Івано-Франківський національний медичний університет, Івано-Франківськ, Україна*

В даній роботі було приготовлено перовскитний матеріал $LaMnO_3$ за допомогою золь-гель методу за участі автогоріння. Згідно Х-променевого фазового аналізу встановлено, що отриманий матеріал складається з однієї фази $LaMnO_3$ (просторова група Pm-3m). Середній розмір ОКР досліджуваного матеріалу 24 нм. За наближенням, що частинки сферичної форми розрахований середній розмір частинки становить 40 - 60 нм. Питома площа поверхні матеріалу складає 42 $м^2/г$. Здійснено елекрохімічні дослідження з використанням нанорозмірного порошку $LaMnO_3$ у якості катодного матеріалу для електрохімічних конденсаторів. Досліджуваний матеріал $LaMnO_3$ показав питому ємність 40 Ф/г при розряді джерела до 1 В.

Ключові слова: золь-гель метод, структура перовскиту, KOH електроліт, питома ємність.